J Solid State Electrochem (2012) 16:1121–1132
DOI 10.1007/s10008-011-1502-9

ORIGINAL PAPER

A novel coprecipitation method towards the synthesis of $Ni_xMn_xCo_{(1-2x)}(OH)_2$ for the preparation of lithium metal oxides

Isadora Rodrigues · Joseph Wontcheu · Dean D. MacNeil

Received: 21 March 2011 / Revised: 30 June 2011 / Accepted: 3 July 2011 / Published online: 22 July 2011

Abstract A series of mixed metal hydroxide ($Ni_xMn_xCo_{(1-2x)}(OH)_2$) precursors for the preparation of lithiated mixed metal oxides ($LiNi_xMn_xCo_{(1-2x)}O_2$) were prepared using a novel coprecipitation approach based on the thermal decomposition of urea. Three different methods were used to achieve the temperature required to decompose urea and subsequently precipitate the hydroxides. The first two methods consisted of either a hydrothermal or microwave-assisted hydrothermal synthesis at 180 °C and elevated pressures. The final method was an aqueous reflux at 100 °C. A complete series (x=0.00–0.50) was prepared for each method and fully characterized before and after converting the materials to lithiated metal oxides ($LiNi_xMn_xCo_{(1-2x)}O_2$). We observed the formation of a complex structure after the coprecipitation of the hydroxides. Scanning electron micrographs images demonstrate that the morphology and particle size of the hydroxide particles varied significantly from x=0.00–0.50 under hydrothermal synthesis conditions. There is also a significant change in particle morphology as the urea decomposition method is varied. The X-ray diffraction profiles of the oxides synthesized from these hydroxide precursors all demonstrated phase pure oxides that provided good electrochemical performance.

Introduction

Rechargeable lithium-ion batteries are the main power source for most high-end portable electronic devices. Currently, many of the major lithium-ion battery manufacturers use $LiCoO_2$ as the positive electrode material due to its ease of fabrication, high energy density, and excellent cycle life. However, there has been a push to replace $LiCoO_2$ because of its elevated production costs and safety concerns about its reactivity [6, 15, 16, 27]. A major research direction has been to partially substitute the Co in $LiCoO_2$ with other transition metals such as Ni and Mn. These so-called mixed metal oxides have been able to provide cathode materials with high capacity, good cycle life, and lower production costs [2, 9–11, 16, 25]. They have also started to appear as the cathode material in commercial cells [14].

Mixed metal hydroxides ($Ni_xMn_xCo_{(1-2x)}(OH)_2$) are used as precursors for the fabrication of electrochemical active lithiated mixed metal oxides ($LiNi_xMn_xCo_{(1-2x)}O_2$). One of the difficulties presented by these hydroxides is the low particle density obtained by the traditional synthesis method [2, 21]. If one were able to produce more dense materials this would lead directly to more dense electrode films and a battery with more energy. The typical synthesis method used consists of the coprecipitation of a mixture of metal salts within a basic solution [11]. There are numerous articles which have reported on various strategies to increase particle density during the coprecipitation of the hydroxides, such as novel synthetic procedures, cation substitutions, metal doping, or modifications to the synthetic procedure during the oxidation to the electrochemically active-lithiated material [2, 6, 22, 26].

In our previous work, we applied different postsynthetic treatments to mixed metal hydroxides obtained by the traditional coprecipitation method [18]. In the present article, we will report a novel synthetic approach, based on the thermal decomposition of urea at elevated temperature, towards the coprecipitation of mixed metal hydrox-

I. Rodrigues · J. Wontcheu · D. D. MacNeil (✉)
Département de chimie, Université de Montréal,
Montréal, QC H3T 1J4, Canada
e-mail: dean.macneil@umontreal.ca

ides, $Ni_xMn_xCo_{(1-2x)}(OH)_2$. As the urea decomposes, the pH of the solution increases leading to the precipitation of the hydroxides from solution. In the traditional coprecipitation method, hydroxides are immediately precipitated when mixed with the basic solution contrary to the precipitation from urea decomposition which takes place when the solution containing the metal salts and urea reach a temperature higher than 90 °C. Thus, all precursors are in the solution state at room temperature and this could lead to a more homogenous precipitation of $Ni_xMn_xCo_{(1-2x)}(OH)_2$ compared to the traditional technique. Moreover, the elevated temperature and increased pressure represent additional parameters not available to the traditional method that could improve the morphology of product and increase the density of the final oxide. This could lead to increased energy density for the cathode electrode.

The traditional coprecipitation method (rapid introduction of a solution of mixed metals into a solution of high pH) results in the rapid saturation of hydroxide once the precipitating agent (OH^-) is readily consumed in the solution. Even in an excess of hydroxide, this typically results in a solution containing a wide particle size distribution and particles with low tap density [13, 23]. The thermal decomposition of urea (reaction scheme below) takes place at temperatures greater than 90 °C [4, 13, 17, 20, 23],

$$NH_2CONH_2 + H_2O \xrightarrow{\Delta} 2NH_3 + CO_2.$$

It represents an alternative precipitation route that has not been investigated for mixed metal hydroxides as precursors for the synthesis of lithiated oxides and could result in more homogenous precipitation with the possibility to obtain smaller particle size distribution, since the nucleation step can be separated from particle growth. In the traditional coprecipitation method, the saturation of the precipitating agent is achieved rapidly leading to the continuous nucleation, growth, and aggregation of particles, resulting in a precipitate with a wide size distribution [23].

The decomposition of urea was previously demonstrated to be a successful precipitation route to metal carbonates [23], various hydroxide phases [4, 13] and, recently, Recham et al. used urea decomposition for the hydrothermal synthesis of $LiFePO_4$ [17]. The main difficulty with the hydroxides, which were prepared previously utilizing the thermal decomposition of urea, is the complex phase obtained from the resultant product. The layered structure of these hydroxides favors the intercalation of ions and molecules within their structure. As a result, the structural analyses of the metal hydroxides prepared using this method is more complex than that of the hydroxides obtained by the traditional coprecipitation method. Dixit et al. reported previously on the synthesis of Co and Ni hydroxides from the decomposition of urea for application as electrode material in alkaline secondary batteries. In their work, it was found that the structure of the synthesized α-hydroxides contained many intercalated NH_3 molecules [4].

Experimental

Preparation

$Co(NO_3)_2{\cdot}6H_2O$ (98%), $Ni(NO_3)_2{\cdot}6H_2O$ (98%), $Mn(NO_3)_2{\cdot}6H_2O$ (98%), NH_2CONH_2, and $LiOH{\cdot}H_2O$ (98%) (Aldrich) were used as starting materials and all solutions were prepared in distilled and degassed water. $Ni_xMn_xCo_{(1-2x)}(OH)_2$ (x=0.00, 0.05, 0.15, 0.30, 0.45, and 0.50) were prepared by a precipitation method based on the thermal decomposition of urea. An aqueous solution containing the mix metal salts with the desired stoichiometry (0.4 M) and NH_2CONH_2 (1.2 M) was prepared and stirred for several minutes. The initial pH value was ~5. Three different routes were developed to achieve the temperature for the thermal decomposition of urea and subsequent precipitation of the hydroxides. The first route consisted of a hydrothermal treatment in which the aqueous solution of the metal salts and urea was transferred into a Teflon container and placed within a sealed digestive vessel (Parr). The vessel was then placed in an oven at 180 °C for 5 h. In the second route, a microwave-assisted hydrothermal treatment was applied. Here, the solution was sealed in closed Teflon liners, which were placed in a turntable for uniform heating within a microwave digestion system (MARS5, CEM). The system operated at a frequency of 2.45 GHz and a power of 1,200 W. The temperature of the microwave was ramped rapidly to 180 °C and kept under these hydrothermal conditions for 15 min. For the third route, the aqueous solution was heated under reflux conditions at 100 °C for 5 h. The pH at the end of all of these reactions was ~7. A traditional coprecipitation reaction was also prepared for comparison by following methods described previously in the literature (metal solution dripped slowly into a solution of high pH) [10, 26]. In all cases, the precipitate products were rinsed several times with distilled water and dried overnight under dry air. The final lithiated oxide, $LiNi_xMn_xCo_{(1-2x)}O_2$, was prepared by mixing the dry hydroxide precursors with an excess (3%) amount of LiOH. After pelletizing, it was heated in air at 500 °C for 3 h, ground, a new pellet formed, and then heated at 900 °C for 3 h followed by a quench cooling (between large copper plates).

Characterization

The crystalline phases of samples were determined by X-ray diffraction (XRD, Bruker D8 Advance) using Cu Kα

radiation with a step size of 0.025° and step time of 15 s in the range of 15–60° or 20–80°. The lattice parameters were refined through Rietveld analysis using the integrated X-ray powder diffraction software package TOPAS Version 3.0. An elemental analysis was carried out on all samples (EAS 1108, Fisions Instruments).

Scanning electron micrographs (SEM) were carried out on a Hitachi S-4300 microscope. Thermal gravimetric analysis (TGA) measurements were performed under a flowing He gas with a TA Instrument thermogravimetric analyser (SDT600) at 15 °C/min from room temperature to 500 °C. Electrochemical evaluations on the lithium metal oxide were performed by combining the oxide with 10% of a conductive carbon (Super-P Li, Timcal) and 10% polyvinylidene difluoride (5.5% in N-methylpyrroldinone (NMP)) with an excess of NMP to make a slurry. The slurry (80% active) was deposited on a carbon-coated Al foil using a doctor blade. The slurry was then dried at 70 °C and electrodes 13 mm in diameter were cut for cell assembly in standard 2032 coin-cell hardware (Hohsen) using a single lithium metal foil as both counter and reference electrode and a Celgard 2200 separator. Cells were assembled in an argon-filled glove box using 1 M $LiPF_6$ in ethylene carbonate/diethyl carbonate (3:1 by vol) electrolyte. Electrochemical evaluations were performed by charging and discharging between 2.2 and 4.2 V using a current rate of 5 mA g^{-1} for the first five cycles and a current of 30 mA g^{-1} for the next 50 cycles at 30 °C on a BT-2000 electrochemical station (Arbin).

Results and discussion

Coprecipitation of mixed metal hydroxides based on the thermal decomposition of urea

At room temperature, a solution-containing urea (NH_2CONH_2) has a pH value of approximately 5. An increase in the pH of the solution is observed at elevated temperature as urea begins its decomposition near 90 °C [17]. Urea decomposes yielding NH_3 into the reaction medium and the pH of the solution increases. Here, the elevated temperature was achieved through three different heating methods and then applied towards the synthesis of $Ni_xMn_xCo_{(1-2x)}(OH)_2$ hydroxides with a stoichiometry of x=0.00–0.50.

Figure 1 shows the X-ray diffraction patterns of all hydroxides obtained with the three different precipitation techniques. We can observe the formation of numerous Bragg diffraction peaks that cannot be indexed with the theoretical pattern expected and demonstrated previously in the literature for $Ni_xMn_xCo_{(1-2x)}(OH)_2$. This difference may be related to the layered structure of the hydroxide and the nature of molecules or ions incorporated from the urea decomposition. In fact as urea decomposes at elevated temperature, it produces numerous ions and molecules such as: CNO^-, HNCO, CO_2, HCO_3^-, NH_4^+, and NH_3 [13, 20, 23]. This complex decomposition scenario can cause the precipitation of metals in compositions other than hydroxides or the incorporation of these various ions within the interlayer spacing of the hydroxide. In any event, we can

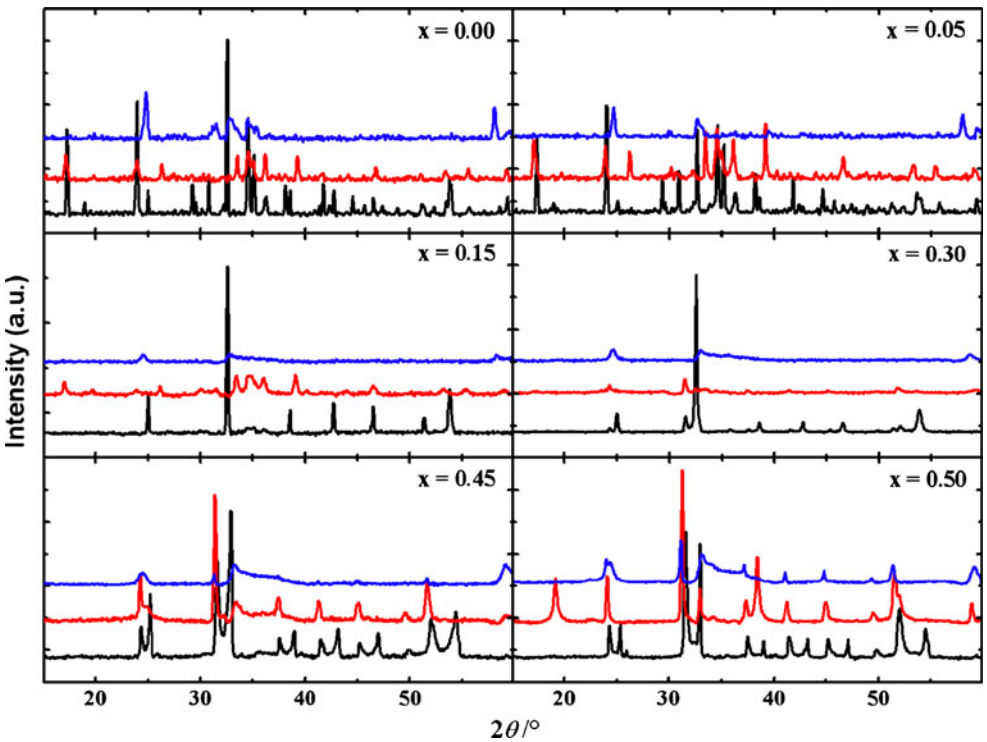

Fig. 1 XRD profiles of $Ni_xMn_xCo_{(1-2x)}(OH)_2$ synthesis based on urea decomposition for the indicated value of x (*bottom black line* under hydrothermal conditions, *middle red line* microwave-assisted hydrothermal, and *top blue line* reflux)

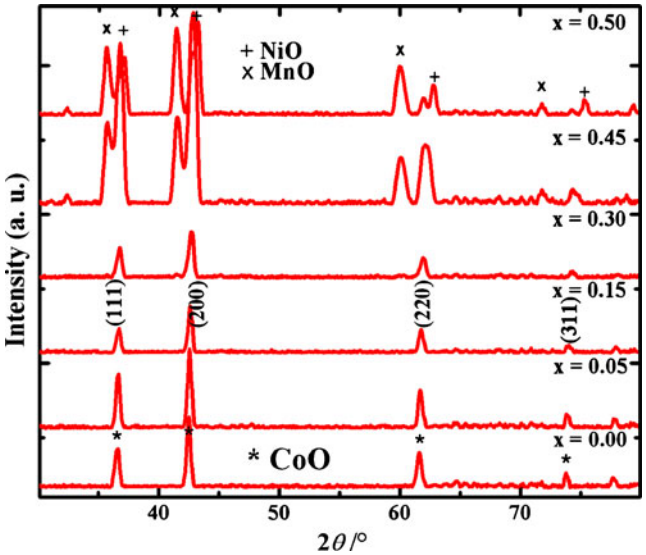

Fig. 2 XRD profiles of $Ni_xMn_xCo_{(1-2x)}(OH)_2$ synthesized using the decomposition of urea under hydrothermal conditions for 24 h

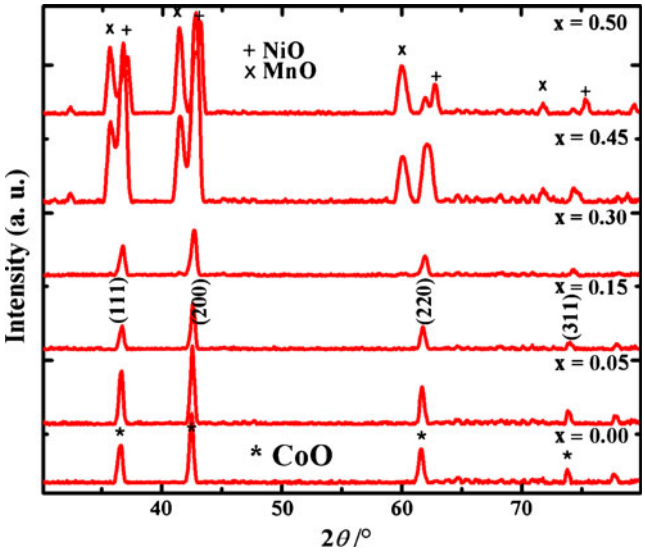

Fig. 4 XRD profiles of $Ni_xMn_xCo_{(1-2x)}(OH)_2$ synthesized using the decomposition of urea via hydrothermal conditions after heating to 500 °C in He

see interesting features from the XRD patterns shown in Fig. 1. If we consider the hydrothermally precipitated material (black lines in Fig. 1), the phases with x=0.00 and 0.05 exhibit more complex powder patterns with numerous peaks positions. As x increase to 0.15 and 0.30, several peaks vanished and finally when the concentration of Ni and Mn are higher than Co ($x \geq 0.30$), all peaks seem to be split in two. In general, the crystallinity of the material improves with the time spent at elevated temperatures. In Fig. 1, the more intense and well-defined peaks are obtained for the hydrothermally precipitated samples (black line in Fig. 1) compared to samples precipitated with the assistance of microwave (red line in Fig. 1). It is even clearer when compared to samples prepared under reflux (blue line in Fig. 1). The complicated diffraction pattern and numerous structural or phase possibilities for these samples have hindered their complete structural characterization. For the sake of simplicity, the samples will continue to be named hydroxides for the remainder of the manuscript although they are likely to contain a mixture of hydroxides with various intercalated species.

We believe that prolonged exposure to elevated temperatures eliminates structural defects that are readily apparent at shorter reaction times, thus hydrothermal syntheses were performed with a longer reaction time of 24 h. Figure 2 shows the XRD diffraction pattern obtained

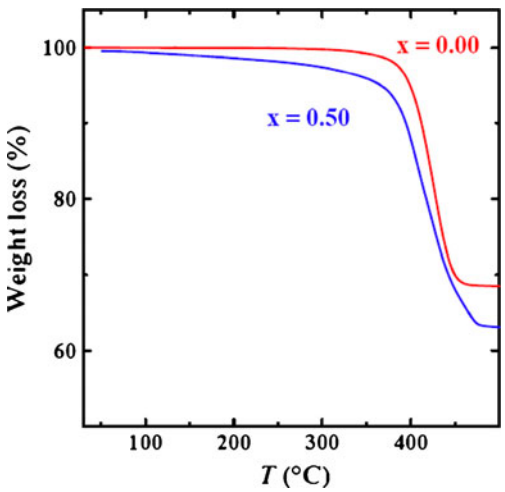

Fig. 3 TGA measurements (15 °C/min) for $Ni_xMn_xCo_{(1-2x)}(OH)_2$ synthesized using the decomposition of urea via the hydrothermal method (*top red line*, x=0.00; *bottom blue line*, x=0.50)

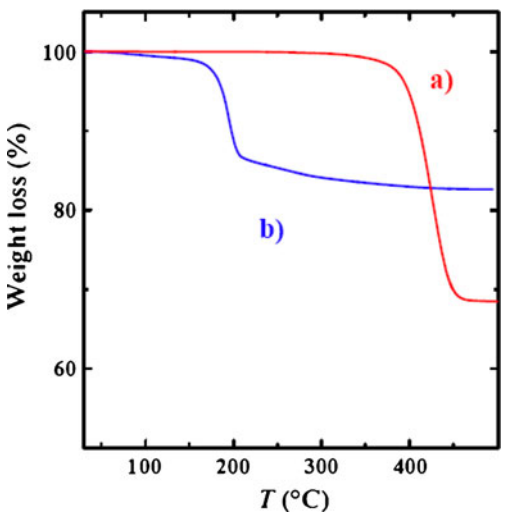

Fig. 5 TGA measurements (15 °C/min) for $Ni_xMn_xCo_{(1-2x)}(OH)_2$ synthesized using the decomposition of urea via the hydrothermal method (*top red line*) and synthesized by the traditional coprecipitation method (*bottom blue line*) (x=0.00)

Table 1 Amount (%) of nitrogen, carbon, and hydrogen in samples prepared by hydrothermal precipitation

	x in $Ni_xMn_xCo_{1-2x}(OH)_2$	N (%)	C (%)	H (%)
Urea decomposition under hydrothermal conditions	0.00	0.02	7.10	0.62
	0.05	0.04	6.41	0.76
	0.15	0.05	9.93	0.19
	0.30	0.07	9.71	0.22
	0.45	0.14	8.78	0.58
	0.50	0.14	8.62	0.64
Traditional coprecipitation	0.50	0.06	0.00	0.36
Traditional+hydrothermally treated	0.50	0.01	0.02	1.24

from samples with x=0.00, 0.30, and 0.50 when reacted under hydrothermal conditions for 24 h. These can be compared to those shown in Fig. 1 where the synthesis took place over 5 h. As samples are exposed to elevated temperature for longer periods of time, several of the Bragg peaks disappeared, while others become more well defined, indicating a reduction in defects as compared to the samples in Fig. 1.

In order to aid in the structural identification of the obtained material, a heating step was performed within a thermogravimetric analyzer. Samples were heated to 500 °C within the TGA under a He atmosphere. According to the TGA results in Fig. 3, the synthesized hydroxides decompose in one stage near 400 °C independent of the concentrations of Ni and Mn in the hydroxide. We therefore assume that the water and any intercalated ions are likely removed at the same time. Figure 4 shows the XRD diffraction pattern of the different compositions after the TGA. For x=0.00, there is the formation of a pure CoO phase, as shown in the XRD. As Ni and Mn are introduced into our samples (increasing x) and heated to 500 °C in He there is a change in the diffraction pattern to what is probably a mixture of CoO, MnO, and NiO phases [4, 7, 8]. When x=0.45, the diffraction pattern presents a significant change compared to samples with x<0.45 and its main

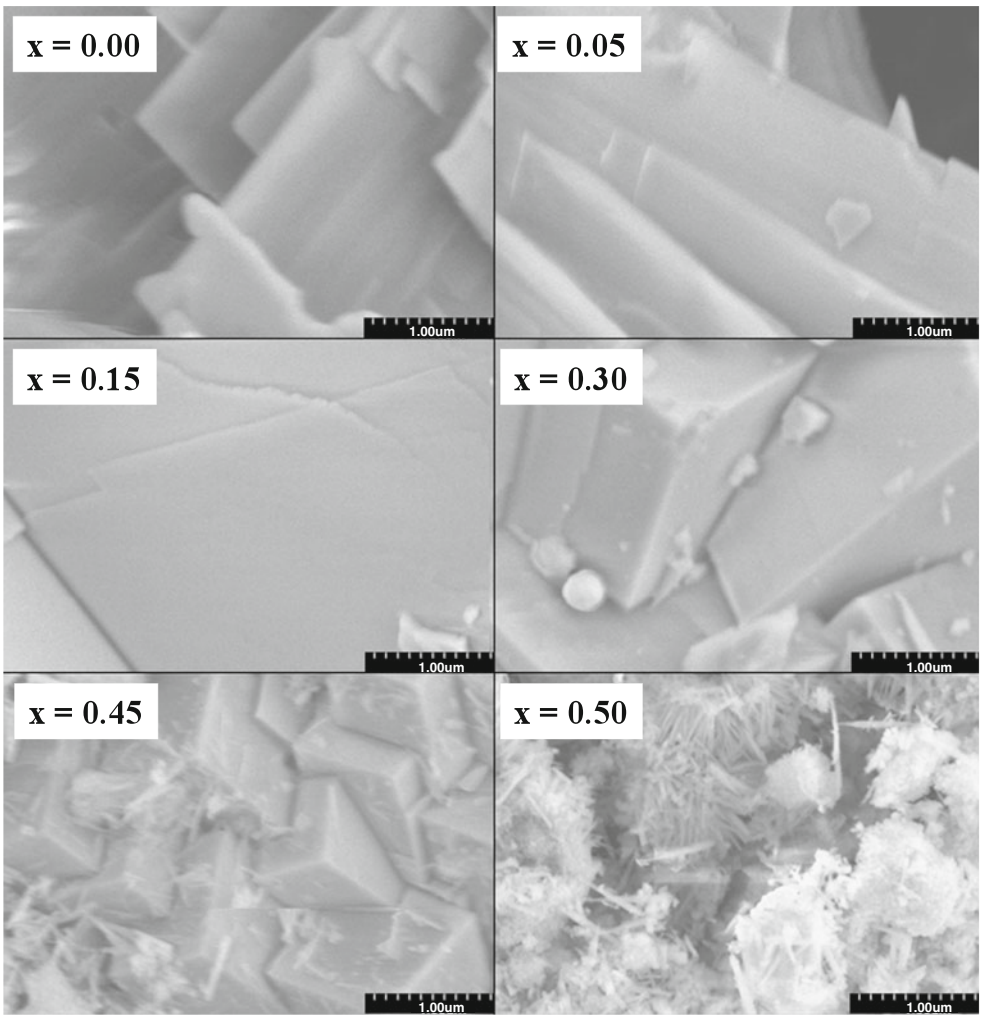

Fig. 6 SEM images of $Ni_xMn_xCo_{(1-2x)}(OH)_2$ synthesized using the decomposition of urea via the hydrothermal method

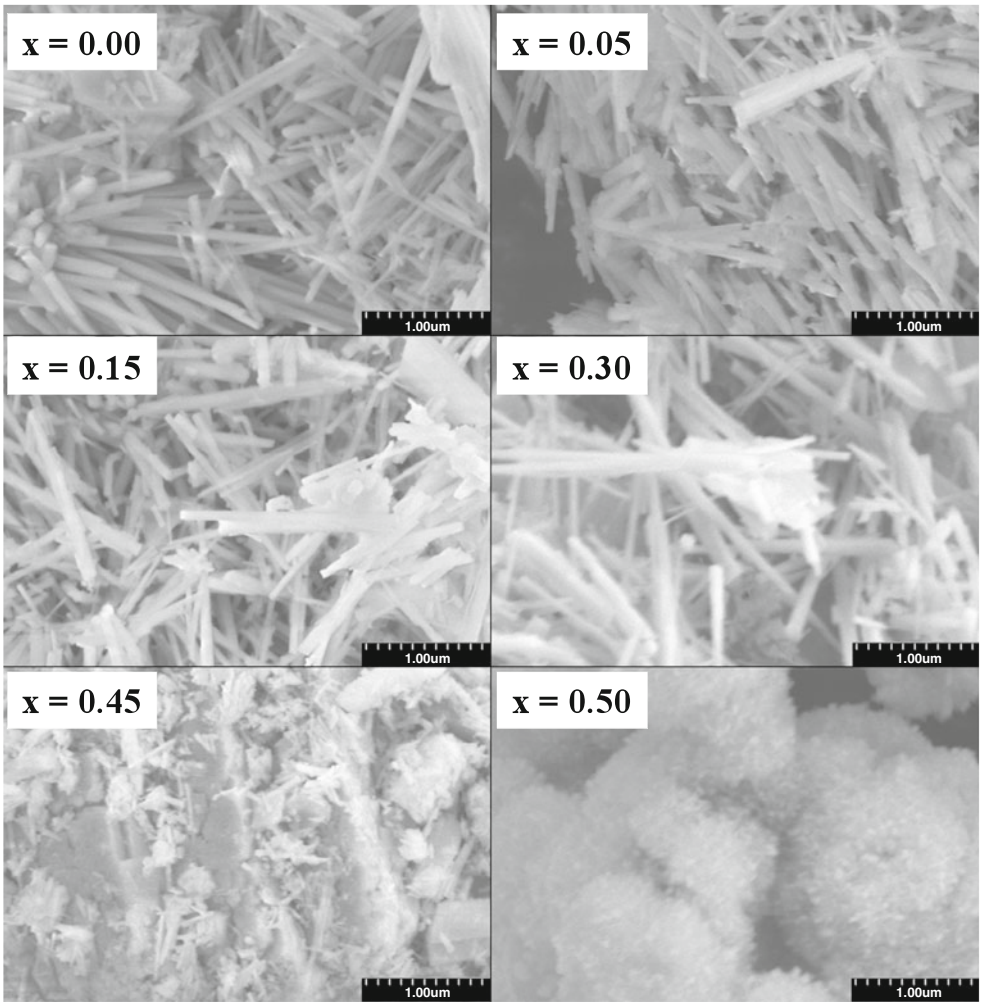

Fig. 7 SEM images of $Ni_xMn_xCo_{(1-2x)}(OH)_2$ synthesized using the decomposition of urea under microwave-assisted hydrothermal conditions

peaks are related to the formation of NiO and MnO. This result is expected as the molar ratio of Co in sample with $x \geq 0.45$ is very small and will only result in a small amount of CoO. Dixit et al. observed similar diffraction patterns for nickel hydroxide heated in He atmosphere [4]. It is interesting to note that the weight loss increases with the amount of Ni and Mn in the sample (Fig. 3), while the temperature of decomposition is only slightly affected. This may indicate that hydroxides with a higher Ni and Mn content have a higher concentration of intercalated ions or molecules. Only two samples are presented in Fig. 3 for simplicity but the other samples do not deviate from the trend shown in Fig. 3.

A comparison between the TGA profiles of the hydroxides prepared by the traditional coprecipitation method and that based on the thermal decomposition of urea (hydrothermal) is shown in Fig. 5 (for $x=0.00$). The weight loss is significantly increased for the sample originating from the urea precipitation compared to the traditional coprecipitation method. This is due to the larger amount of intercalated water molecules or ions within the sample synthesized using the decomposition of urea. According to the TGA results, samples prepared with urea decompose at ~400 °C (Fig. 5a) while samples prepared by the traditional coprecipitation method decompose at ~200 °C. The weight loss in both samples is associated with the release of absorbed water, conversion of the hydroxides into oxides, and decomposition of ions and/or molecules intercalated within the hydroxides layers. The interlayer species are more tightly bound within the hydroxides layers of the samples precipitated from the thermal decomposition of urea resulting in improved thermal stability for these samples. This increase in thermal stability with the binding of interlayer species in hydroxides is common and has been described before [1, 3, 24].

Table 1 shows the results of the elemental analysis on the hydrothermally precipitated hydroxide samples to demonstrate the presence of intercalated ions and/or molecules within the layered hydroxide. The presence of NH_3 within similar materials has been reported previously in the literature [4]. The amount of nitrogen within these hydroxides increases as x increases to 0.50, which is in

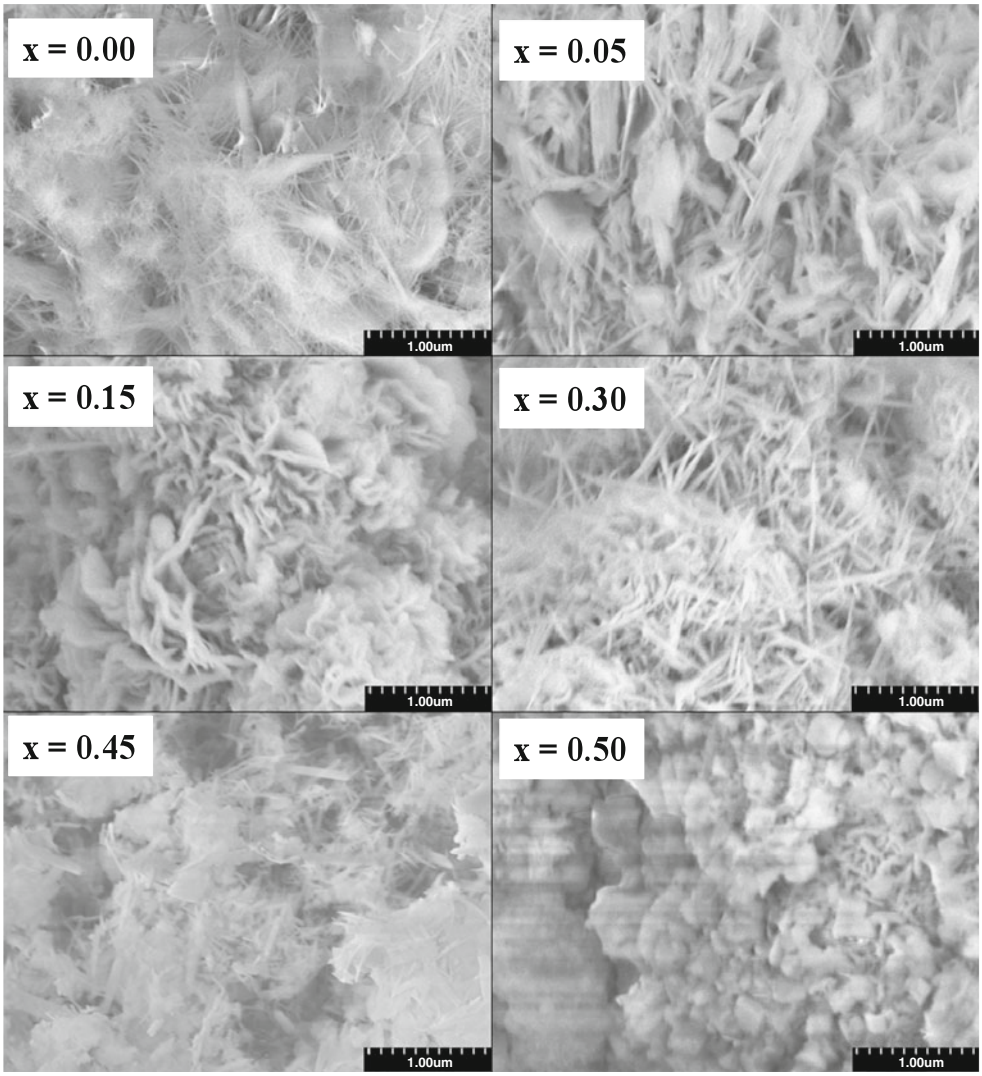

Fig. 8 SEM images of $Ni_xMn_xCo_{(1-2x)}(OH)_2$ synthesized using the decomposition of urea under reflux conditions

agreement with the increase in weight loss observed in the TGA experiments when x increases to 0.50. Hydroxides prepared through the traditional coprecipitation method have a smaller content of nitrogen when compared to the hydroxides, of the same composition, prepared through the thermal decomposition of urea. The presence of nitrogen is even smaller if we compare them to the samples prepared by the traditional coprecipitation method using a hydrothermal postsynthetic treatment. The nitrogen present in the sample prepared by the traditional method comes from the nitrate in the precursor metal salts. Thus, we can consider that the increase in nitrogen content of samples from urea decomposition compared to traditional method is due to the presence of NH_3 generated by the decomposition of urea.

The carbon content was also analyzed. The difference between the carbon content for samples prepared by the traditional method compared to the urea-based samples is even more pronounced than with nitrogen. If we consider samples with a stoichiometry of x=0.50, a carbon content of 8.6% is obtained for the sample prepared with urea compared to 0.02% (detection limit of our machine) for the samples prepared by a traditional coprecipitation method followed by a hydrothermal postsynthetic treatment. The higher amount of carbon likely originates from ions and molecules intercalated into the hydroxides (ex.: CO_2, HCO_3^-, NHCO, and NCO^-) that are produced during the decomposition of urea. The elemental analysis provides valuable information about the possible ions and molecules intercalated within the hydroxides; however, it is not possible to determine the exact composition of these species. Numerous ions and molecules can be intercalated within the structure of phases prepared here and this is a likely reason as to why the amount of N, C, and H measured for these samples are not increasing homogenously with increasing values of x.

SEM was used to determine the morphology of the samples. Figure 6 shows images of hydroxides obtained

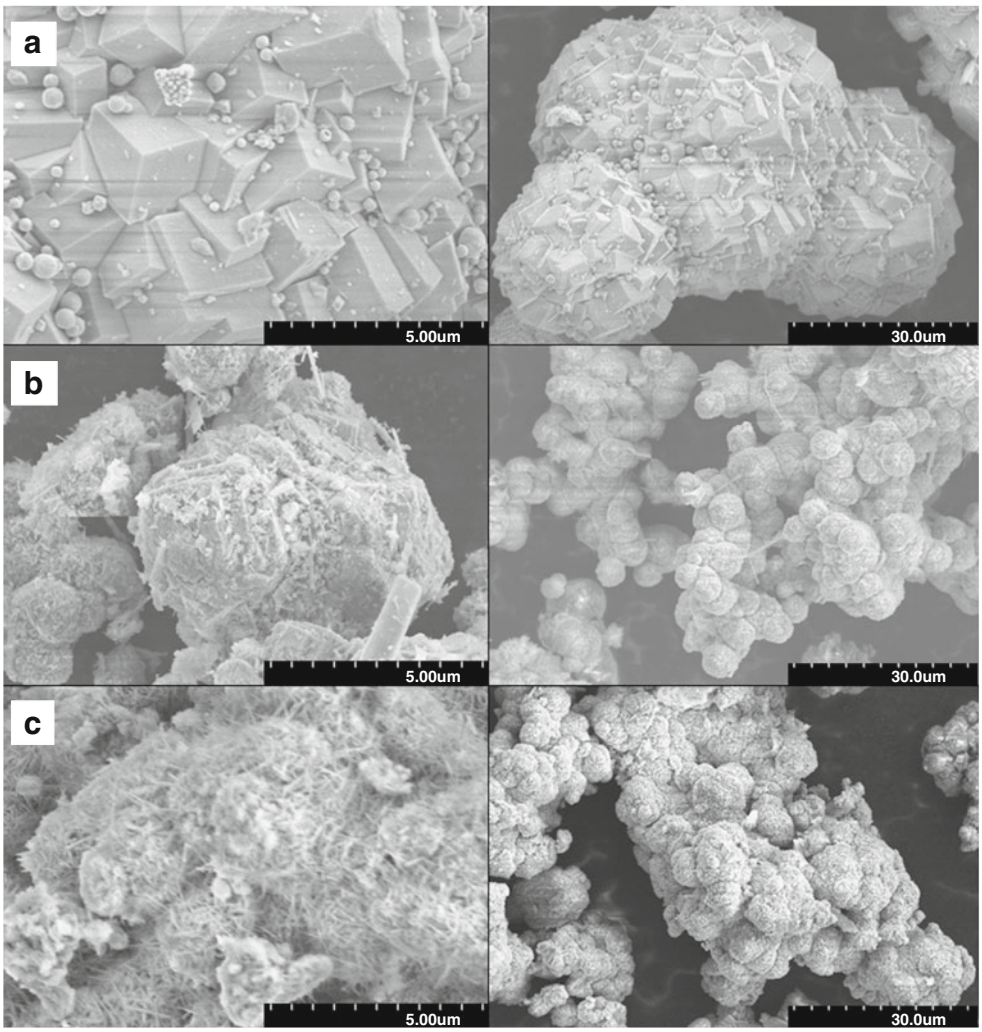

Fig. 9 Comparison of particle size and morphology for $Ni_xMn_xCo_{(1-2x)}(OH)_2$. **a** Prepared under hydrothermal conditions, **b** microwave-assisted hydrothermal conditions, and **c** reflux conditions. *Left column scale bar*, 5 μm; *right column*, 30 μm; x=0.30

with the hydrothermal/urea technique. When x=0.00 and 0.05 a clear layered morphology is visible. This trend tends to change to larger square particles when x=0.30 and 0.45 and finally at x=0.50, the square particles become covered by fine needle-like particles in a pattern that can suggest a biphasic material, however, more detailed analysis would be necessary to clarify this point. All the hydroxides shown in Fig. 6 have a larger particle size compared to the samples prepared by the traditional coprecipitation method without any postsynthetic treatment [2, 18]. Figures 7 and 8 show the SEM images of the samples prepared with the microwave-assisted hydrothermal and reflux techniques, respectively.

The hydroxides synthesized from these methods have smaller particle size than those presented in Fig. 6. The samples from the microwave-assisted synthesis (Fig. 7) from x=0.00–0.30 have a very well-formed needle morphology while at x=0.45 and 0.50 the needles disappear and a more random morphology is observed. The hydroxides synthesized under reflux conditions (Fig. 8) do not present a well-formed morphology. The lack of well-formed particles is directly related to the XRD results presented in Fig. 1 where well-formed crystallized products are observed for the hydrothermal sample contrary to samples synthesized using either the microwave or reflux methods which clearly show a loss of crystallinity (Fig. 1).

In Fig. 9, we compare the images of the samples (x=0.30) from the three different heating techniques at two different magnifications. Particles obtained from the hydrothermally prepared samples (Fig. 9a) are larger when compared to either the microwave (Fig. 9b) or reflux (Fig. 4.9c) method. The increase in particle size is due to the increase in time at high temperature. The time at higher temperature also plays an important role in the crystallinity of the final material as observed in Fig. 1. On the right side of the Fig. 9a, we present a smaller magnification level to provide a better view of the general morphology of the agglomerates. We can see that all hydroxides, regardless of preparative method, present a spherical global morphology. The microwave and reflux techniques generate a cotton ball morphology formed by the agglomeration of many fine needle-like particles while the large spherical morphology

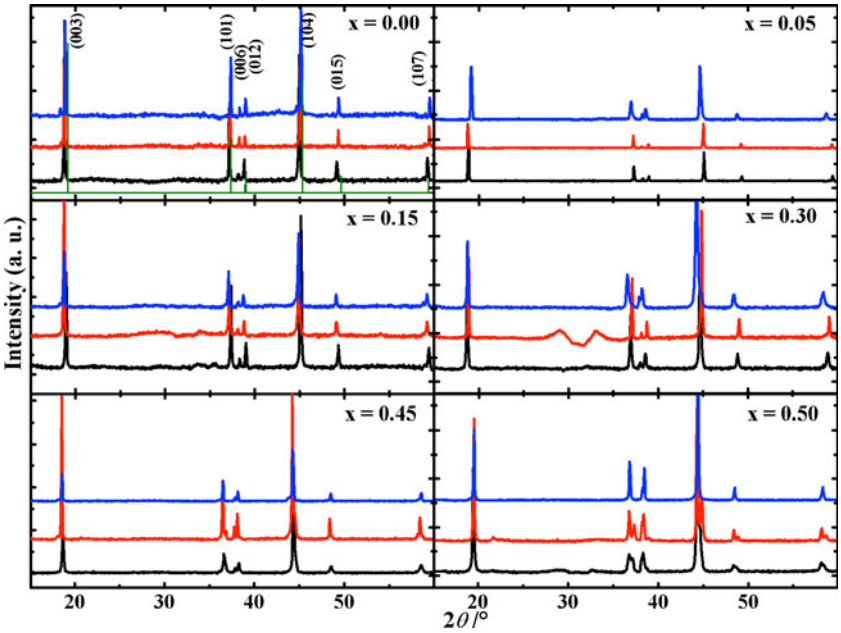

Fig. 10 XRD profiles of $LiNi_xMn_xCo_{(1-2x)}O_2$ (*bottom black line* from precursor prepared under hydrothermal conditions, *middle red line* from precursor prepared under microwave-assisted hydrothermal conditions, *top blue line* from precursor prepared under reflux conditions and the *green lines* in the x=0.00); quadrant is a representation of the Bragg peaks, with indicated Miller indices, for $LiCoO_2$ that can be used as a reference

from the hydrothermal method is formed by the agglomeration of large square particles.

Lithium mixed metal oxides

For application within lithium-ion batteries, these mixed metal hydroxides need to be oxidized into lithiated oxides. It has been found previously that the morphology of the precursor hydroxide has a significant effect on the ability to produce the optimal dense, spherical-lithiated oxides [2, 25, 27]. Thus, it is important to fully investigate various synthetic methods for the synthesis of these hydroxides with the purpose of obtaining dense oxides, which will lead to dense electrodes and higher energy density batteries. Figure 10 shows the XRD patterns of the oxides produced from the various hydroxide precursors described above.

The obtained powder patterns (Fig. 10) compare well with those in the literature for $LiNi_xMn_xCo_{(1-2x)}O_2$ phases. This suggests that the novel synthesis approach for the coprecipitation of hydroxides precursors does not seem to affect the

Table 2 Lattice parameters and cell unit volume of $LiNi_xMn_xCo_{(1-2x)}O_2$, indexed using the R3m space group

	x in $LiNi_xMn_xCo_{1-2x}O_2$	a (Å)	c (Å)	V (Å^3)
Hydrothermal	0.00	2.859 (2)	14.230 (2)	100.7 (4)
	0.05	2.864 (4)	14.258 (4)	101.3 (4)
	0.15	2.867 (1)	14.274 (4)	101.6 (3)
	0.30	2.870 (2)	14.277 (1)	101.8 (2)
	0.45	2.876 (2)	14.279 (1)	102.3 (3)
	0.50	2.893 (1)	14.284 (2)	103.5 (4)
MW-hydrothermal	0.00	2.888 (3)	14.299 (3)	103.2 (2)
	0.05	2.892 (3)	14.298 (2)	103.6 (4)
	0.15	2.896 (4)	14.288 (1)	103.6 (3)
	0.30	2.897 (2)	14.299 (3)	103.9 (2)
	0.45	2.900 (1)	14.283 (4)	104.0 (3)
	0.50	2.905 (1)	14.309 (3)	104.6 (2)
Reflux	0.00	2.886 (2)	14.256 (2)	102.8 (2)
	0.05	2.886 (3)	14. 259 (4)	103.0 (3)
	0.15	2.890 (2)	14.269 (3)	103.2 (3)
	0.30	2.898 (2)	14.274 (2)	103.8 (3)
	0.45	2.908 (4)	14.285 (3)	102.2 (2)
	0.50	2.910 (1)	14.294 (1)	104.6 (3)

Table 3 Cation compositions in $LiNi_xMn_xCo_{(1-2x)}O_2$ phases determined from X-ray data for samples synthesized under traditional coprecipitation followed by hydrothermal treatment

x	0.00	0.05	0.15	0.30	0.45	0.5
x'	0.00	0.047 (2)	0.152 (3)	0.297 (1)	0.450 (3)	0.496 (3)

x is the nominal composition and x' is obtained from the Rietveld refinement of the X-ray data (standard deviations are in parenthesis)

structure or crystalinity of the oxides despite the presence of intercalated ions and molecules within our hydroxides. Those species are probably decomposed in gaseous forms when the hydroxides are exposed to high temperature in air. Table 2 presents the lattice parameters of all the oxides indexed using the α-$NaFeO_2$ type structure (trigonal *R3m*). As expected, with increasing Mn and Ni concentration, the *a* and *c* lattice parameters as well as the unit cell volume, *V*, increases with the value of *x* in all cases which is not surprising as the ionic radius of the substituted Ni^{2+} (0.69 Å) ions is larger than that of Co^{3+} (0.54 Å) [5, 12, 19]. The ionic radius of Mn^{4+} (0.53 Å) is about the same size as that of Co^{3+} and the increase in the lattice parameters of $LiNi_xMn_xCo_{(1-2x)}O_2$ when *x* increases is highly related to the insertion of Ni^{2+} into the lattice [1]. The lattice parameters of oxides prepared with precursors from the microwave and reflux method are slightly larger compared to those from the hydrothermally prepared samples. This difference is in the same order of magnitude as the standard deviation obtained during our lattice parameters determination and may not be related to foreign phases present in the oxides. As the use of coprecipitation synthetic methods often leads to deviations from nominal cation compositions, we have included in Table 3 a comparison of the expected substituted ion concentration and that determined via Rietveld analysis of the powder data for the phase synthesized under the traditional coprecipitation followed by hydrothermal treatment. It is clear that a very good correlation is obtained with only a minor variation.

Figure 11 shows the SEM images of the $LiNi_xMn_xCo_{(1-2x)}O_2$ prepared from hydroxide precursors based on the urea decomposition using the hydrothermal method (Fig. 11a), microwave-assisted hydrothermal (Fig. 11b), and reflux (Fig. 11c) methods. Each sample is shown with two

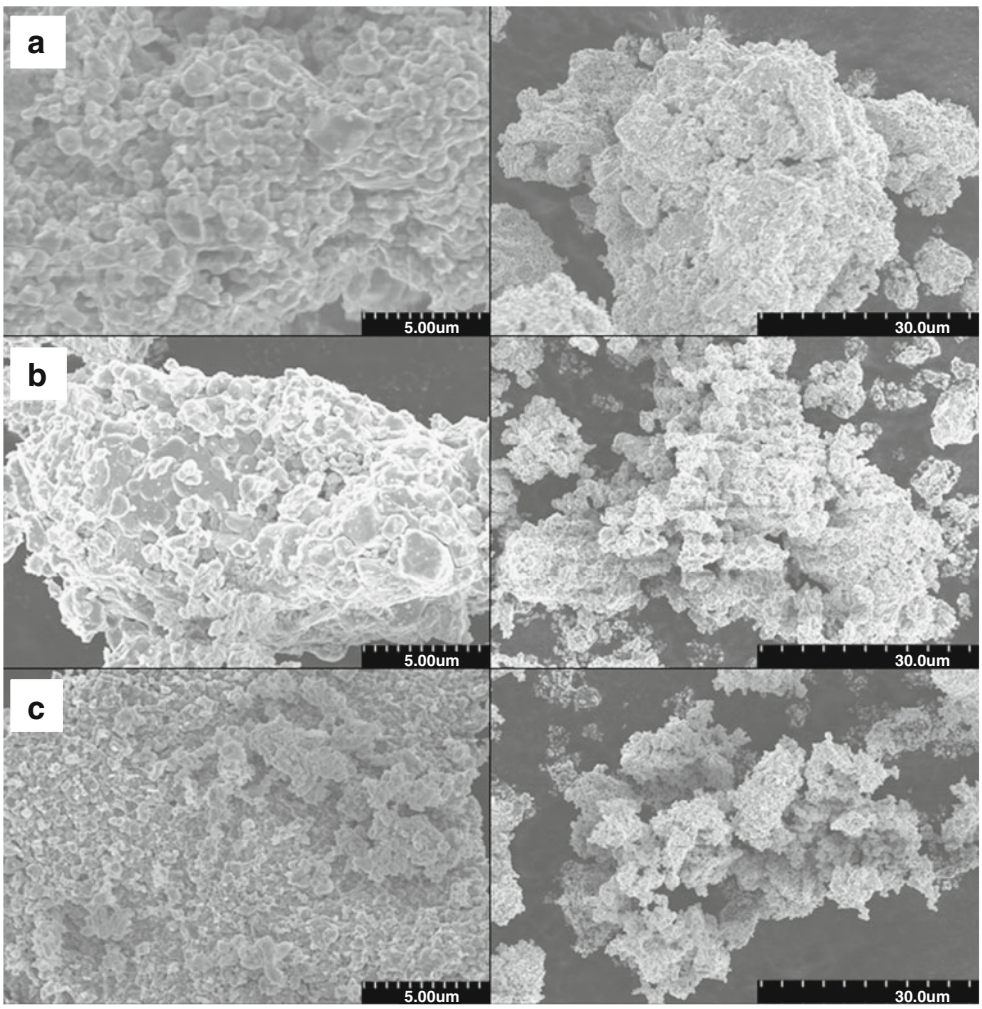

Fig. 11 SEM images of $LiNi_xMn_xCo_{(1-2x)}O_2$ (x=0.30) prepared with hydroxide precursors **a** prepared under hydrothermal conditions, **b** microwave-assisted hydrothermal conditions, and **c** reflux conditions. *Left column scale bar*, 5 μm; *right column*, 30 μm

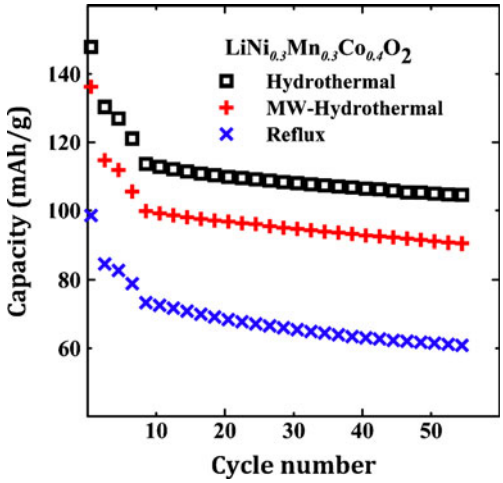

Fig. 12 Capacity vs. cycle number for $LiNi_xCo_{1-2x}Mn_xO_2$ (x=0.15) charged to 4.2 V. Comparison of different methods used to achieve the required temperature to decompose urea. Hydrothermal condition (*black square*), microwave-assisted hydrothermal (*red positive sign*), and reflux (*blue multiplication symbol sign*). The charge–discharge curves consist of five cycles at a rate of 5 mA g^{-1} followed by 50 cycles at 30 mA g^{-1}

different magnifications (left scale bar, 5 μm; right scale bar, 30 μm; x=0.30). While the particle size of the precursor hydroxides showed a significant increase for the urea decomposition under hydrothermal conditions with respect to the other methods, the particle size of all oxides, regardless of the particle size of the precursor, are similar, but the particles from the hydrothermal method tend to agglomerate into larger agglomerates.

The capacity retention (capacity versus cycle number), for the electrodes of oxides from precursors hydroxide based on urea decomposition for the three different heating techniques, is shown in Fig. 12 for x=0.30 in $LiNi_xMn_xCo_{(1-2x)}O_2$: hydrothermal (black squares), microwave-assisted hydrothermal (red crosses), and reflux (blue xs). The positive cathode material was cycled at 30 °C between 2.2 and 4.2 V. The first five cycles were charged at a rate of 5 mA g^{-1}, while the remaining cycles were charged at a rate of 30 mA g^{-1}. Electrodes prepared with oxides from precursors synthesized using the hydrothermal technique have higher capacity than those obtained from other heating methods. The same trend was found for all Ni and Mn concentrations.

Figure 13 presents electrochemical performance of the samples: prepared either by the traditional coprecipitation method or based on urea decomposition (hydrothermally prepared). The oxides prepared from precursors obtained using the decomposition of urea does not result in a large change in electrochemical performance as compared to the traditionally prepared coprecipitation precursors. The electrochemical results of the samples from urea decomposition with $x \geq 0.05$ are very similar to those obtained via the traditional coprecipitation method. Even though the capacity obtained from the urea samples was similar to the oxides prepared with traditional hydroxide precursors, we consider these results as promising as the precipitation based on the thermal decomposition of urea present numerous parameters (such as temperature, pH, time, etc.) that can be explored to improve various electrochemical properties (capacity, cycle life, and tap density) of the final oxide. Further research into this reaction schemes are underway within our research group. The capacity of $LiCoO_2$ (from the traditional coprecipitation precursor)

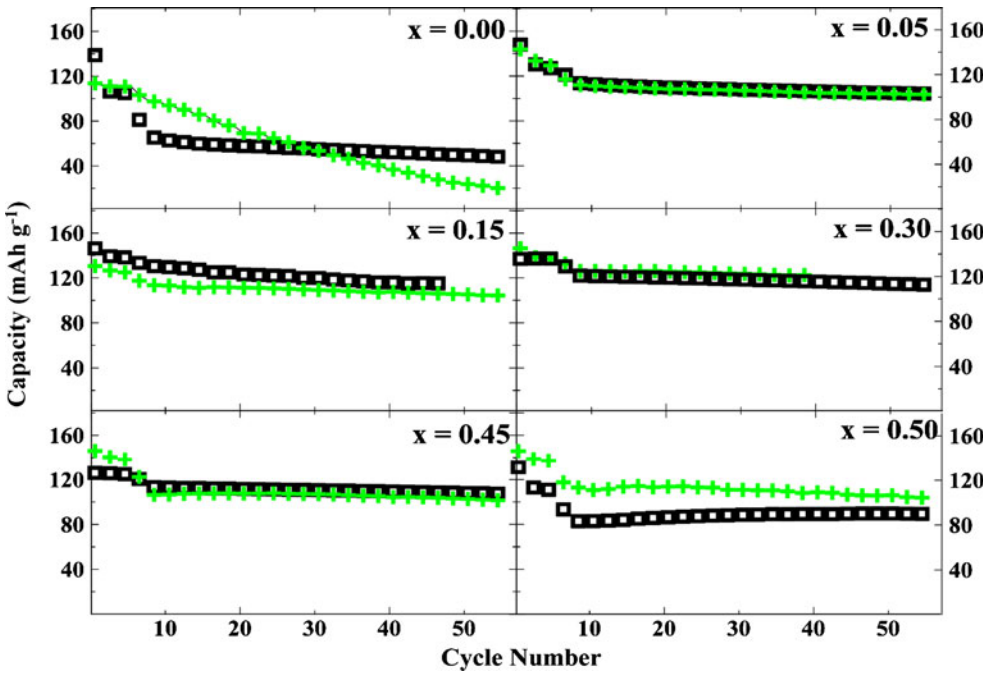

Fig. 13 Comparison of the capacity vs. cycle number for $LiNi_xCo_{1-2x}Mn_xO_2$ charged to 4.2 V with hydroxides precursors prepared from the coprecipitation under hydrothermal conditions for the decomposition of urea (*black circle*) to hydroxides prepared using the traditional coprecipitation method (*green positive sign*). The charge–discharge curves consist of five cycles at a rate of 5 mA g^{-1} followed by 50 cycles at 30 mA g^{-1}

cycled at 4.2 V decreases drastically with increasing cycle number. This characteristic is typical of $LiCoO_2$ synthesized using the standard coprecipitation technique, but the synthesis of $LiCoO_2$ using the thermal decomposition of urea provides a significant improvement in capacity retention compared to standard coprecipitation technique. Further improvements (for example, particle size and morphology improvements) are necessary to increase the capacity of $LiCoO_2$ obtained from urea precipitation to equal the capacity of $LiCoO_2$ synthesized from standard solid-state techniques [1, 18].

Conclusion

$Ni_xMn_xCo_{(1-2x)}(OH)_2$ (x=0.00–0.50) were synthesized using a novel coprecipitation approach based on the thermal decomposition of urea. Three different techniques were used to achieve the required temperature to decompose urea leading to the precipitation of the mixed metal hydroxide: hydrothermal, microwave-assisted hydrothermal, and reflux. To the best of our knowledge, it is the first time that the precursors for mixed metal oxides have been prepared via a latent base. This method can provide an additional control towards the precipitation of the hydroxide and consequently could help in improving the particle size, morphology, and reactivity of the mixed oxide samples. The controlled precipitation at elevated temperature could lead to a more homogenous precipitation of $Ni_xMn_xCo_{(1-2x)}(OH)_2$ compared to the traditional technique. The elevated temperature and pressure used during the precipitation represent additional parameters not available in the traditional method that could also improve the morphology of the hydroxides and increase the density of the final oxide. The density of hydroxide precursors has already demonstrated to be fundamentally important towards the preparation of denser oxides [21]. Therefore, it is important to develop novel synthesis routes and treatments that optimize particle size and morphology.

The time at elevated temperature during synthesis has a significant impact on the crystallinity and morphology of the hydroxides. Samples which were prepared using hydrothermal heating, show larger particle size and greater crystallinity. At longer reaction time (24 h), the hydrothermally prepared samples demonstrate a decrease in the number of defects that are readily apparent in samples with reduced exposure time at high temperature. More experiments are needed to define the optimized scenario concerning synthesis parameters. Samples prepared with all methods and within all stoichiometry ranges were successfully used as precursor for the synthesis of the electrochemically active lithiated mixed metal oxides ($LiNi_xMn_xCo_{(1-2x)}O_2$). Phase pure oxides, with very similar morphology regardless of the particle size and morphology of precursors, were obtained. The electrochemical properties of these samples presented characteristics similar to literature.

References

1. Barbosa CAS, Ferreira AMDC, Constantino VRL (2005) Eur J Inorg Chem 8:1577–1584
2. Barkhouse DAR, Dahn JR (2005) J Electrochem Soc 152:A746–A751
3. del Arco M, Carriazo D, Martín C, Grueso AMP, Rives V (2006) Mater Sci Forum 514–516:1541–1545
4. Dixit M, Subbanna GN, Kamath PV (1996) J Mater Chem 6:1429–1432
5. Jouanneau S, Dahn JR (2003) Chem Matt 15:495–499
6. Jouanneau S, Eberman KW, Krause LJ, Dahn JR (2003) J Electrochem Soc 150:A1637–A1642
7. Kosova NV, Devyatkina ET, Kaichev VV (2007) J Power Sources 174:735–740
8. Kovanda F, Grygar T, Dornicak V (2003) Solid State Science 5:1019–1026
9. Liu Z, Yu A, Lee JY (1999) J Power Sources 81–82:416–419
10. Lu Z, Dahn JR (2001) J Electrochem Soc 148:A237–A240
11. Lu Z, MacNeil DD, Dahn JR (2001) Electrochem Solid-State Lett 12:A200–A203
12. MacNeil DD, Lu Z, Dahn JR (2002) J Electrochem Soc 149: A1332–A1336
13. Marvis B, Akinc M (2006) J Am Ceramic Soc 89:471–477
14. Nagaura T, Tozawa K (1990) Prog Batteries Solar Cells 9:209
15. Ohzuku T, Makimura Y (2001) Chem Lett 30:642–643
16. Ohzuku T, Makimura Y (2001) Chem Lett 30:744–745
17. Recham N, Armand M, Laffont M, Tarascon J-M (2009) Electrochem Solid-State Lett 12:A39–A44
18. Rodrigues I, Wontcheu J, MacNeil DD (2011) (in press)
19. Shannon RD (1976) Acta Crystallogr A32:751–767
20. Shaw WR, Bordeaux JJ (1955) J Am Chem Soc 82:4729–4736
21. van Bommel A, Dahn JR (2009) J Electrochem Soc 156:A362–A365
22. van Bommel A, Dahn JR (2009) Chem Mater 21:1500–1503
23. Vial S, Prevot V, Forano C (2006) J Phys Chem Solid 67:1048–1053
24. Wei M, Xu XY, He J, Rao GY, Yang HL (2006) J Therm Anal Cal 85:795–800
25. Yabuuchi N, Koyama Y, Nakayama N, Ohzuku T (2005) J Electrochem Soc 152:A1434–A1440
26. Zhao X, Zhou F, Dahn JR (2008) J Electrochem Soc 155:A642–A647
27. Zhou F, Zhao X, van Bommel A, Rowe AW, Dahn JR (2010) Chem Mater 22:1015–1021